

Condition Monitoring of Electrolytic Capacitors via ESR Estimation with Recursive Least Squares and Sliding Mode Techniques

J. M. Andrade

*University of Derby, College of Engineering and Technology,
Department of Electronics, Computing and Mathematics, Derby, DE22 3AW, England, U.K.*

Keywords: Condition Monitoring, Capacitor Diagnosis, Capacitor Ageing, Equivalent Series Resistance (ESR), Sliding Mode Differentiator, Robust Exact Differentiation, Recursive Least Squares (RLS).

Abstract: A new on-line electrolytic capacitor condition monitoring approach based on sliding mode concepts and the recursive least squares (RLS) with constant forgetting factor algorithm is proposed in this paper. This scheme involves robust exact differentiation which outperforms the classical differentiator based on linear approximations, when the system is affected by noise. The condition monitoring approach proposed in this paper allows for on-line estimation of the ESR which is considered to be one of the best indicators of capacitor degradation. Computer simulation results, considering a DC-DC buck converter, provide evidence of the effectiveness of the capacitor condition monitoring scheme proposed in this paper.

1 INTRODUCTION

Capacitor failure may be classified into (i) catastrophic failure when a capacitor has completely lost its functionality, for instance, short and open circuit failure modes, and (ii) degradation failure when a gradual deterioration of a capacitor occurs. The causes of the short and open circuit failures are overvoltage, mechanical stress, excessive ripple current, reverse voltage, weak point of electrolytic paper, defective oxide layer, and insufficient connection of tab and terminal part, whereas degradation or wear-out failures are mainly caused by charging and discharging cycles, high operating temperature, overvoltage stress and excessive ripple current (Nichicon Corporation, nd). Capacitor degradation is also known as capacitor ageing.

Electrolytic capacitor degradation results in a gradual increase in the equivalent series resistance (ESR) (i.e. the sum of the resistances associated with the aluminium oxide, electrolyte, paper spacers and electrodes) and also a decrease in capacitance over time. An indication of the condition of a capacitor may be obtained by monitoring these two electrical properties (Abdennadher et al., 2008). The degradation of an electrolytic capacitor is primarily attributed to electrolyte evaporation, leakage current, and internal pressure increase (Alwitt and Hills, 1965) (Wang and Blaabjerg, 2014) (Hewitt et al., 2016). The end-of-

life (EoL) of an aluminium electrolytic capacitor is reached when its capacitance changes by 20% and/or its ESR doubles (Hewitt et al., 2016) (Soliman et al., 2016).

A review of the condition monitoring of capacitors in power converters that summarized different methods for determining the ESR and/or capacitance has been presented in (Soliman et al., 2016), see references therein for details of the different methods. The Kalman filter paradigm (Kalman, 1960) has been applied to the problem of on-line estimation of ESR and/or capacitance, e.g. (Abdennadher et al., 2009) (Celaya et al., 2011). In (Celaya et al., 2011) besides using a Kalman filter, an empirical degradation model was used for prediction of the remaining useful life of electrolytic capacitors. Recursive least squares (RLS) and least mean squares algorithms were considered in (Buiatti et al., 2007a) and (Buiatti et al., 2007b) respectively. Another condition monitoring system based on RLS that also incorporated capacitor ageing models that describe the evolution of ESR and capacitance with respect to temperature, was proposed in (Abdennadher et al., 2008) and (Abdennadher et al., 2009). Application of digital signal processing concepts to the problem of ESR and capacitance estimation are reported in (Amaral et al., 2007) and (Imam et al., 2005). A wide range of experimental methods have also been developed, e.g. (Kulkarni et al., 2010) (Kulkarni et al., 2012) (Hewitt et al., 2016) (Amaral

et al., 2007).

The increase of ESR is considered by many researchers, e.g. (Wang et al., 2012), the best indicator of capacitor degradation. In this regard, an ESR estimation scheme based on sliding mode concepts and the RLS algorithm is proposed in this paper. The sliding mode theory (Shtessel et al., 2014) has extensively been applied to control and estimation/observation problems, and still is a theory under development albeit the sliding mode ideas began in the late 1950s in the Soviet Union. After a relatively extensive literature review, it became noticeable that sliding mode concepts are yet to be applied to the capacitor condition monitoring problem. In this paper, a sliding mode differentiator, which is robust with respect to input noise and exact in their absence (Levant, 1998), is integrated into an ESR estimation scheme for capacitor condition monitoring that also involves the RLS algorithm with forgetting factor.

The main contributions of this paper are: (i) some level on novelty since, to the best knowledge of the author, sliding mode ideas have not been applied to the problem of estimating ESR for capacitor condition monitoring before, (ii) simplicity in terms of its form and design, and relative straightforward implementation at no extra cost since the existing microcontroller, DSP or FPGA devices are already used in many power electronic systems such as power converters, and (iii) on-line nature which allows for real-time capacitor condition monitoring.

2 PROBLEM FORMULATION

The most common type of aluminium electrolytic capacitor consists of two aluminium foils which form the anode and apparent cathode, paper separators, a liquid electrolyte which is the real cathode, an aluminium oxide layer (Al_2O_3) which is the dielectric and of sufficient thickness to withstand the rated voltage of the capacitor, two terminals, and an aluminium can (Alwitt and Hills, 1965).

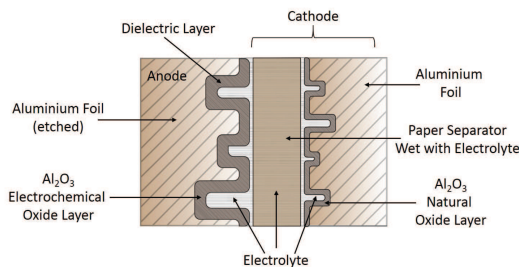


Figure 1: Structure of an electrolytic capacitor element.

The electrolytic capacitor element depicted in Figure 1 may be modelled as the equivalent electric circuit shown in Figure 2. The ideal capacitance is denoted by C_{AK} . The resistance R_p represents the insulation resistance. The resistance R_l corresponds to the series resistance of foils, paper and terminals. The inductance of windings and connections is represented by L .

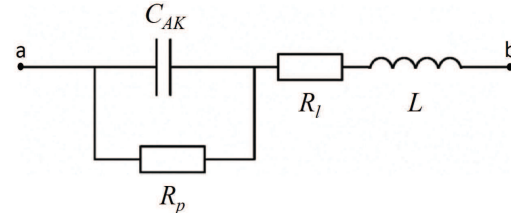


Figure 2: Equivalent electric circuit of an electrolytic capacitor.

The impedance of the equivalent circuit, shown in Figure 2, takes the following form

$$Z_{ab} = R_{ESR} + j\left(\omega L_{ESL} - \frac{1}{\omega C_E}\right) \quad [\Omega] \quad (1)$$

where the equivalent series inductance (ESL) is given by $L_{ESL} = L$ [H], the ESR is given by

$$R_{ESR} = R_l + \frac{R_p}{1 + \omega^2 R_p^2 C_{AK}^2} \quad [\Omega] \quad (2)$$

and the equivalent capacitance is given by

$$C_E = C_{AK} \left(1 + \frac{1}{\omega^2 R_p^2 C_{AK}^2}\right) \quad [\text{F}] \quad (3)$$

Furthermore, the magnitude of the impedance and the resonant frequency are given by

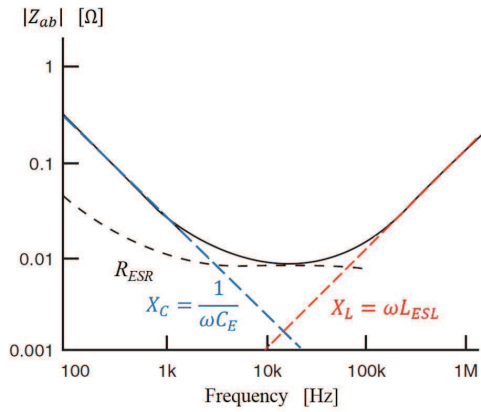
$$|Z_{ab}| = \sqrt{R_{ESR}^2 + \left(\omega L_{ESL} - \frac{1}{\omega C_E}\right)^2} \quad [\Omega] \quad (4)$$

and

$$f_r = \frac{1}{2\pi\sqrt{L_{ESL}C_E}} \quad [\text{Hz}] \quad (5)$$

The impedance characteristics of an electrolytic capacitor is shown in Figure 3. For frequencies $f < f_r$ impedance is dominated by the capacitive reactance $X_C = \frac{1}{\omega C_E}$, whereas for $f > f_r$ the impedance is dominated by the inductive reactance $X_L = \omega L_{ESL}$. Moreover for $f_1 < f < f_2$ the impedance is mainly resistive and hence dominated by R_{ESR} .

Without loss of generality, it is assumed that the power electronics system, on which the condition monitoring approach proposed in this paper will be applied, is a DC-DC Buck converter. Consequently, since DC-DC power converters typically operate at a lower frequency band compared with the resonant frequency defined in (5) and the equivalent series inductance L_{ESL} is relatively small, e.g. in the order of nH,


 Figure 3: Frequency characteristics of $|Z_{ab}|$.

ESL may be neglected. Nevertheless, the switching frequency of the power converter is high enough, i.e. typically in the middle frequency range, for the impedance Z_{ab} to be dominated by R_{ESR} . Note that the switching frequency that will be considered in Section (4) is 10 kHz which means that the impedance Z_{ab} is dominated by R_{ESR} (see Figure 3). Since this will be the case considered in this paper, the equivalent circuit shown in Figure 2 can be simplified as shown in Figure 4.



Figure 4: Simplified equivalent circuit of an electrolytic capacitor.

A widely applied criterion states that the EoL of electrolytic capacitors is reached when its capacitance changes by 20% and/or its ESR doubles (Hewitt et al., 2016) (Soliman et al., 2016). Other criteria are also available. For instance, the military standard MIL-C-62F has been used in (Celaya et al., 2011) to define that the EoF of an electrolytic capacitor is reached if its ESR increases by 280-300% or the capacitance decreases by 20% with respect to the respective pristine condition values.

From the simplified equivalent circuit shown in Figure 4, it follows that the difference of potential between anode and cathode terminals is given by

$$v_{ab}(t) = R_{ESR}(t)i_C(t) + \frac{1}{C_E} \int_0^t i_C(\tau) d\tau \quad (6)$$

which, in turn, yields the following differential equation

$$\begin{aligned} \frac{dv_{ab}(t)}{dt} &= i_C(t) \frac{dR_{ESR}(t)}{dt} + R_{ESR}(t) \frac{di_C(t)}{dt} \\ &+ \frac{1}{C_E} (i_C(t) - i_C(0)) \end{aligned} \quad (7)$$

By defining

$$y_m(t) = \frac{dv_{ab}(t)}{dt} - \frac{1}{C_E} (i_C(t) - i_C(0)) \quad (8)$$

$$\varphi^T(t) = \left[\frac{di_C(t)}{dt} \quad i_C(t) \right] \quad (9)$$

and

$$\vartheta = \left[R_{ESR}(t) \quad \frac{dR_{ESR}(t)}{dt} \right]^T \quad (10)$$

the differential equation given in (7) can be written as a generic linear model (Ljung, 1999) (Mendel, 2008), which is linear in the unknown vector of parameters ϑ , and takes the following form

$$y_m(t) = \varphi^T(t)\vartheta + \eta_m(t) \quad (11)$$

where $\eta_m(t) \in \mathfrak{R}$ denotes the measurement noise.

Since the increase of ESR is the best indicator of capacitor degradation (Wang et al., 2012), the problem to be addressed in this paper is the on-line estimation of the equivalent series resistance $R_{ESR}(t)$ for condition monitoring of electrolytic capacitors through the generic linear model given in (11). This problem will be tackled within the context of a DC-DC converter as in (Buiatti et al., 2007a) (Soliman et al., 2016).

3 PROPOSED SOLUTION

The measurement $y_m(t)$ and the observation vector $\varphi(t)$ of the generic linear model (11) involve the potential difference of the anode-cathode terminals $v_{ab}(t)$ and the capacitor current $i_C(t)$, which are measurable analogue signals, and their first derivatives $\frac{dv_{ab}(t)}{dt}$ and $\frac{di_C(t)}{dt}$ respectively. In this paper, these derivatives will be obtained by using sliding mode differentiators (Levant, 1998). The voltage $v_{ab}(t)$ and current $i_C(t)$ may be affected by noise and hence the classical differentiator based on linear approximations will not produce satisfactory derivatives as will be demonstrated in Section 4.

Although this paper is not concerned with the physical implementation of the proposed solution, two conceptual designs are discussed in the sequel. The scalar and vector signals $y_m(t)$ and $\varphi(t)$ are obtained using (8) and (9), which may be realised using operational amplifiers, and then these signals are sampled at a frequency f_s (in the order of tens or hundreds of kHz) prior to be processed by an RLS-based estimator implemented on a microcontroller, DSP or FPGA. A block diagram of the condition monitoring scheme proposed in this paper is shown in Figure 5.

The proposed solution may also be implemented entirely on a digital programmable device. In this

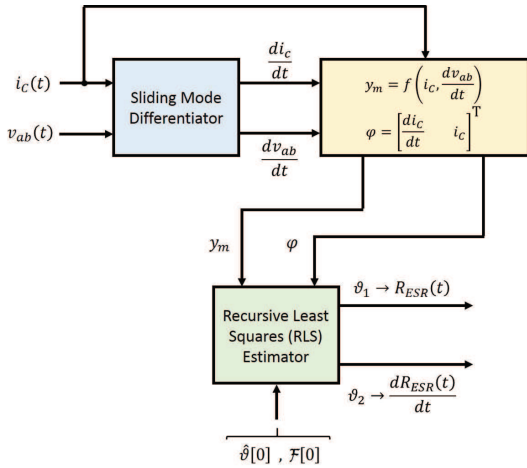


Figure 5: Block diagram of the proposed ESR estimation scheme for electrolytic capacitor condition monitoring.

case, the electrolytic capacitor voltage $v_{ab}(t)$ and current $i_C(t)$ would be sampled and a digital version of the sliding mode differentiators could be adopted. Then, the representation of the signals $y_m[k]$ and $\varphi[k]$ may be realised by software and, of course, the RLS algorithm is also implemented on software.

In what follows, the theory associated with the robust exact differentiator and the RLS estimation algorithm is summarised.

3.1 Sliding Mode Differentiator

The sliding mode robust exact differentiator (Levant, 1998) corresponds to a second-order sliding mode (2-sliding mode) technique. In order to introduce the sliding mode differentiator used in the ESR estimation scheme, some definitions and main theoretical results are provided for the sake of mathematical rigour and completeness. Consider the space of measurable functions (or signals) bounded on an interval $[a, b]$ denoted by $\mathcal{M}_{[a, b]}$ and to which the continuous-time input signal $s_i(t)$ belongs to. It is also assumed that $\|s_i(t)\| = \sup|s_i(t)|$.

A first-order differentiator \mathcal{D} is said to be an exact differentiator if its output signal, i.e. $\hat{s}_i(t) = \frac{ds_i(t)}{dt}$, matches the time derivative of the input signal $\dot{f}(t)$. Note that the order of the differentiator is the order of the derivative produced. The robustness of the differentiator is an important feature since in real-world applications the input signal may be corrupted with relatively small high-frequency noise, which always exists and may have a large derivative. In this regard, if the output signal of a differentiator \mathcal{D} tends uniformly to $\mathcal{D}s_i(t)$ as the input signal tends uniformly to $s_i(t)$, then the differentiator \mathcal{D} is said to be a robust differentiator. Moreover, if a differentiator \mathcal{D} has

both the exactness and robustness properties defined previously, then it is said to be a correct differentiator.

For a practical real-time differentiator, as the ones required by the electrolytic capacitor condition monitoring for generating $\frac{dv_{ab}(t)}{dt}$ and $\frac{di_C(t)}{dt}$, it is assumed that the input signal $s_i(t)$ is a measurable locally bounded function defined on the interval $[0, \infty)$ and consists of a base signal involving a derivative with a Lipschitz constant $\mathcal{L} > 0$ and noise (Levant, 1998).

Define the auxiliary differential equation

$$\dot{x}(t) = y(t) \quad (12)$$

and the following first-order real-time robust exact differentiator, which guarantees that $x(t) \rightarrow s_i(t)$, i.e. $x(t) - s_i(t) = 0$ (Levant, 1993) (Levant, 1998):

$$y(t) = z(t) - \lambda|x(t) - s_i(t)|^{1/2} \text{sgn}(x(t) - s_i(t)) \quad (13)$$

$$\dot{z}(t) = -\kappa \text{sgn}(x(t) - s_i(t)) \quad (14)$$

where the signal $y(t)$ is the output of the differentiator, and scalars $\lambda, \kappa \in \mathbb{R}^+$ are selected by the designer for the convergence of $y(t)$ to $\dot{s}_i(t)$. Sufficient conditions will be provided below.

The solution of equations (12)-(14) has to be interpreted in the sense of *Filippov's* theory (Filippov, 1988). Following the description presented in (Levant, 1998), define

$$\Phi(\kappa, \lambda, \mathcal{L}) = |\Psi(t_*)| \quad (15)$$

where $(\Sigma(t), \Psi(t))$ is the solution of the system

$$\dot{\Sigma} = -|\Sigma|^{1/2} + \Psi \quad (16)$$

$$\dot{\Psi} = \begin{cases} -\frac{1}{\lambda^2}(\kappa - \mathcal{L}) & -|\Sigma|^{1/2} + \Psi > 0 \\ -\frac{1}{\lambda^2}(\kappa + \mathcal{L}) & -|\Sigma|^{1/2} + \Psi \leq 0 \end{cases} \quad (17)$$

$$\Sigma(0) = 0 \quad (18)$$

$$\Psi(0) = 1 \quad (19)$$

where $\kappa > \mathcal{L}$, $\lambda \neq 0$ and $t_* = \inf\{t \mid t > 0, \Sigma(t) = 0, \Psi(t) < 0\}$ with $t_* < \infty$. Note that the function $\Phi(\kappa, \lambda, \mathcal{L})$ has to be determined through computer simulations. The convergence criterion of $y(t)$ to $\dot{f}(t)$ is stated in the following theorem.

Theorem 3.1 (Levant, 1998): *Let $\kappa > \mathcal{L} > 0$, $\lambda > 0$ and $\Phi(\kappa, \lambda, \mathcal{L}) < 1$. Then, provided $f(t)$ has a derivative with Lipschitz constant \mathcal{L} ($f \in W(\mathcal{L}, 2)$ where $W(\mathcal{L}, 2)$ is the set of all input signals such that their first derivatives have a Lipschitz constant $\mathcal{L} > 0$), the equality $y(t) = \dot{f}(t)$ holds identically after a finite-time transient process.* ■

In (Levant, 1998), the following sufficient conditions for the convergence of $y(t)$ to $\dot{f}(t)$ are given

$$\kappa > \mathcal{L}, \quad (20)$$

$$\lambda^2 \geq 4\mathcal{L} \frac{\kappa + \mathcal{L}}{\kappa - \mathcal{L}}. \quad (21)$$

Now consider the following assumptions: $\kappa > \mathcal{L} > 0$, $\lambda > 0$, and $\Phi < 1$.

Theorem 3.2 (Levant, 1998): *Let $s_i(t) = s_{i_0}(t) + \eta(t)$ be the input signal, where $s_{i_0}(t)$ is a differentiable base signal, $s_{i_0}(t)$ has a derivative with Lipschitz constant $\mathcal{L} > 0$, and $\eta(t)$ is the noise satisfying $|\eta(t)| \leq \varepsilon$. Then, there exists a constant $b > 0$ dependent on $(\kappa - \mathcal{L})/\lambda^2$ and $(\kappa + \mathcal{L})/\lambda^2$ such that after finite time the inequality*

$$|y(t) - \dot{s}_{i_0}(t)| < \lambda b \varepsilon^{1/2} \quad (22)$$

is satisfied.

If κ and λ are chosen such that $\kappa = \zeta_1 \mathcal{L}$ and $\lambda = \zeta_2 \mathcal{L}^{1/2}$ respectively, then the inequality

$$|y(t) - \dot{s}_{i_0}(t)| < \tilde{b} \mathcal{L}^{1/2} \varepsilon^{1/2} \quad (23)$$

holds for some $\tilde{b}(\zeta_1, \zeta_2) > 0$. ■

A discrete-time version of the sliding mode differentiator can be obtained by applying the one-step Euler method to (12)-(14) (Livne and Levant, 2014):

$$x[k+1] = x[k] + T_s z[k] - \lambda_d T_s |e[k]|^{1/2} \text{sgn}(e[k]) \quad (24)$$

$$z[k+1] = z[k] - \kappa_d T_s \text{sgn}(e[k]) \quad (25)$$

where

$$e[k] = x[k] - s_i[k] \quad (26)$$

and T_s is the sample time. The positive scalars λ_d and κ_d are the design parameters of the sliding mode differentiator.

3.2 Recursive Least Squares Estimator

Since the parameter of interest for electrolytic capacitor condition monitoring is $R_{ESR}(t)$, which is a slowly time-varying parameter, RLS with exponential forgetting is integrated into the condition monitoring scheme proposed in this paper. The calculations involved in this RLS method are given in the following theorem.

Theorem 3.3 (Recursive Least Squares with Exponential Forgetting): *Given the estimation linear model*

$$\hat{y}_m[k] = \Phi^T[k] \hat{\vartheta}[k] + \eta_m[k] \quad (27)$$

where $\hat{y}_m \in \mathfrak{R}$ is the model output, $\Phi \in \mathfrak{R}^r$ is the regressor vector which is a known deterministic vector (the components of Φ are said to be the regression variables), and $\hat{\vartheta} \in \mathfrak{R}^r$ is the parameter vector estimate. Provided that $\hat{\vartheta}[0] = \hat{\vartheta}_0$ and $\mathcal{P}[0] = \mathcal{P}_0$, the least squares estimate of the vector of unknown parameters $\hat{\vartheta}$ satisfies the following recursive equations:

$$\hat{\vartheta}[k] = \hat{\vartheta}[k-1] + \mathcal{K}[k] (y_m[k] - \Phi^T[k] \hat{\vartheta}[k-1]) \quad (28)$$

where

$$\begin{aligned} \mathcal{K}[k] &= \mathcal{P}[k] \Phi[k] \\ &= \mathcal{P}[k-1] \Phi[k] (\lambda_{RLS} + \Phi^T[k] \mathcal{P}[k-1] \Phi[k])^{-1} \end{aligned} \quad (29)$$

and

$$\mathcal{P}[k] = \frac{1}{\lambda_{RLS}} (\mathbf{I} - \mathcal{K}[k] \Phi^T[k]) \mathcal{P}[k-1] \quad (31)$$

and minimises the cost function

$$J(\hat{\vartheta}, \tau) = \frac{1}{2} \sum_{k=1}^{\tau} \lambda_{RLS}^{\tau-k} (y_m[k] - \Phi^T[k] \hat{\vartheta}[k])^2 \quad (32)$$

where the forgetting factor λ_{RLS} is such that $0 < \lambda_{RLS} < 1$. ■

The initial value $\mathcal{P}(0)$ is chosen as

$$\mathcal{P}(0) = \gamma_{RLS} I \quad (33)$$

where $\gamma_{RLS} \in \mathfrak{R}$ is a large number.

The gain vector $\mathcal{K}[k]$ in Theorem (3.3) provides a proportional correction to the difference between the actual measurement $y_m[k]$ and the estimate output $\hat{y}_m[k]$ based on the previous parameter estimate $\hat{\vartheta}[k-1]$. Moreover, cost function (32) involves a time-varying weighting of the squared of this difference, i.e. $e_y^2 = (y_m[k] - \Phi^T[k] \hat{\vartheta}[k-1])^2$, through the factor $\lambda_{RLS}^{\tau-k}$. Thus, it is possible to give more emphasis to recently observed measurements rather than to older data.

Note that $\lambda_{RLS} = 1$ corresponds to the fundamental RLS algorithm in which all data are weighted equally and the algorithm has an infinite memory length (Zhuang, 1998). The choice of λ_{RLS} is a trade-off between tracking and noise sensitivity (Ljung, 1999). That is, less weight to older measurements, i.e. λ_{RLS} small, means that older data is forgotten faster. However, the algorithm is more sensitive to noise. Usually, the forgetting factor λ_{RLS} is chosen from the interval $[0.95, 0.99]$. In (Isermann and Münchhof, 2011), it is suggested that λ_{RLS} has to be selected as follows: (i) a small λ_{RLS} if the rate of change of the parameter is large and only small noise is allowed; (ii) a large λ_{RLS} if the rate of change of the parameter is small and noise can be larger.

4 DESIGN AND SIMULATION

In this section, a DC-DC buck converter (see Figure 6) with nominal parameter values given in Table 1 is considered. For this purpose, a model of the entire system (i.e. DC-DC converter and condition monitoring scheme) was implemented on MATLAB/Simulink.

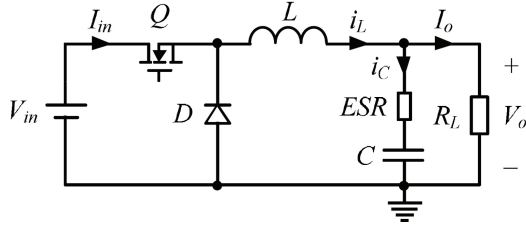


Figure 6: DC-DC buck converter schematic.

Table 1: Nominal parameter values for the DC-DC Buck Converter.

V_{in}	L	r_L	C	ESR	R_L	f_{sw}	DS	V_0
[V]	[H]	[$\mu\Omega$]	[mF]	[m Ω]	[Ω]	[kHz]	[%]	[V]
200	0.21	68.7	1.041	25	1.584	10	50	100

Sliding mode differentiators for estimation of $\frac{dv_{ab}(t)}{dt}$ and $\frac{di_C(t)}{dt}$ were designed and their gains are shown in Table 2.

Table 2: Sliding mode differentiator gains.

	Differentiator 1	Differentiator 2
λ	420×10^3	8.40×10^{12}
κ	4.7250×10^{12}	2.2×10^6

The RLS with forgetting factor algorithm, presented in Theorem 3.3, was implemented as a MATLAB function. The following parameter values were used on the computer simulations: $\lambda_{RLS} = 0.99$, $\vartheta(0) = [0 \ 0]^T$ and $\mathcal{F}(0) = 100I$. A large constant forgetting factor has been selected since ESR is a slowly time-varying parameter. Furthermore, this large λ_{RLS} allows for a reduced estimation noise. The sample time considered for the RLS estimator was 100 kHz, i.e. $10f_{sw}$. Regarding the MATLAB/Simulink model configuration parameters, they were set as follows: ode1 (Euler) solver with fixed-step size (fundamental sample time) of 1×10^{-9} seconds.

An experiment involving a simulated change in the ESR value (see, for example, the black colour curve in Figure 12) was carried out. Note that in order to emulate the electrolytic capacitor degradation, the ESR value was gradually increased. Moreover, the capacitor voltage and current measurements were corrupted by noise. In this respect, two different uniformly distributed random signals were injected to the capacitor voltage and current measurements, i.e. $\eta_{v_{ab}}$: amplitude = $\pm 1 \times 10^{-3}$ [V] and seed = 2, and η_{i_C} : amplitude = $\pm 5 \times 10^{-3}$ [A] and seed = 4. The sample time of 1×10^{-6} seconds was used for both signals.

The results obtained with the proposed scheme are compared against the following classical first-order linear approximation differentiator (LAD):

$$G(s) = \frac{s}{100 \times 10^9 s + 1} \quad (34)$$

This differentiator was used alongside the very same RLS with forgetting algorithm used for the sliding mode based scheme. In this paper, this approach will be called the classical scheme or method.

A detail of the performance of the DC-DC buck converter is shown in Figure 7.

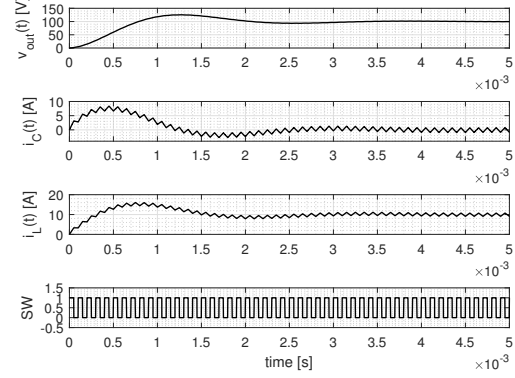
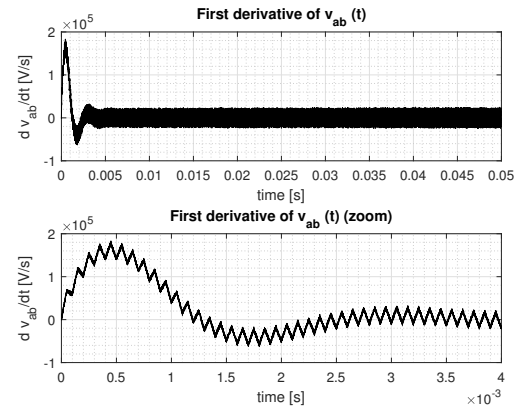


Figure 7: DC-DC buck converter dynamic response (zoom).

The first derivatives $\frac{dv_{ab}(t)}{dt}$ and $\frac{di_C(t)}{dt}$, obtained with the sliding mode differentiators, are shown in Figures 8 and 9 respectively. On the other hand, the same derivatives but produced by the classic LAD are depicted in Figures 10 and 11. The better performance of the sliding mode differentiator is evident from these graphs. This will become even more evident when assessing the performance of both condition monitoring schemes later on.

The time evolution of the true and estimated ESR, using the proposed scheme and the classical method, are shown in Figure 12 and 13. Furthermore, the corresponding errors $e_{ESR_{SMS}} = |R_{ESR} - \hat{R}_{ESR_{SMS}}|$ and $e_{ESR_{CM}} = |R_{ESR} - \hat{R}_{ESR_{CM}}|$ are provided in Figure 14. The performance of the classical method (CM) is indeed unacceptable because it cannot estimate the ESR in the case of noisy measurements and hence


 Figure 8: First derivative of the capacitor voltage, i.e. $\frac{dv_{ab}(t)}{dt}$, obtained with the sliding mode differentiator.

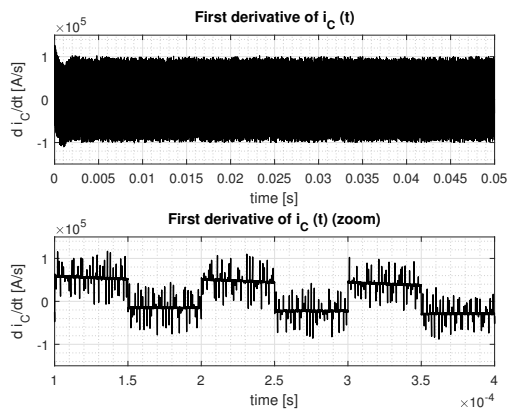


Figure 9: First derivative of the capacitor current, i.e. $\frac{di_c(t)}{dt}$, obtained with the sliding mode differentiator.

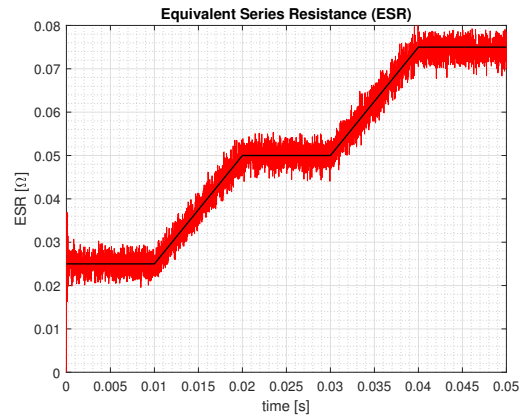


Figure 12: True and estimated ESR obtained with the proposed scheme.

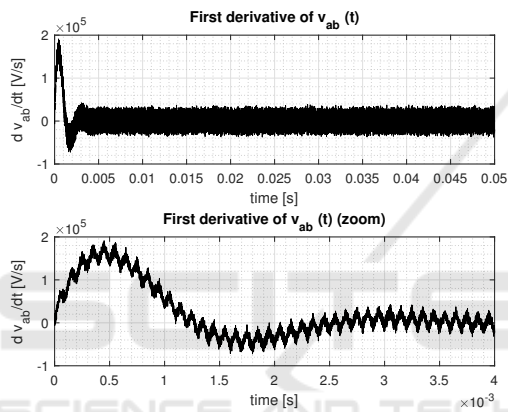


Figure 10: First derivative of the capacitor voltage, i.e. $\frac{dv_{ab}(t)}{dt}$, obtained with the classical first order LAD.

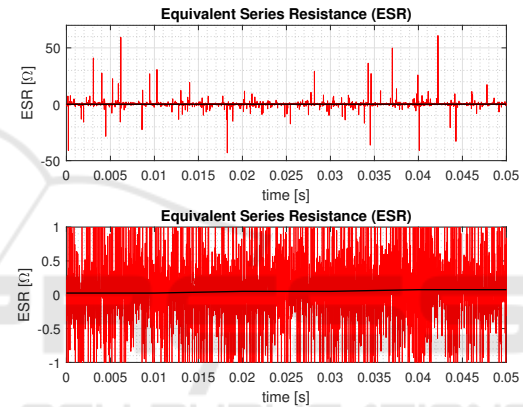


Figure 13: True and estimated ESR obtained with the classic method.

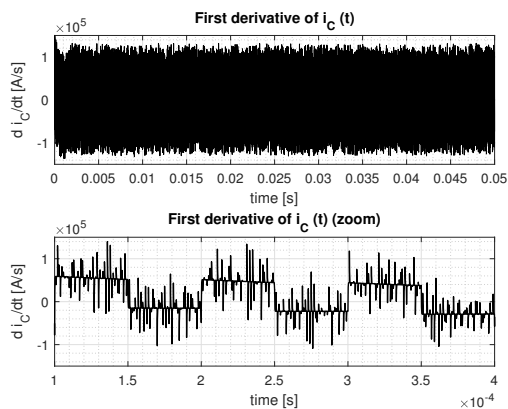


Figure 11: First derivative of the capacitor current, i.e. $\frac{di_c(t)}{dt}$, obtained with the classical first order LAD.

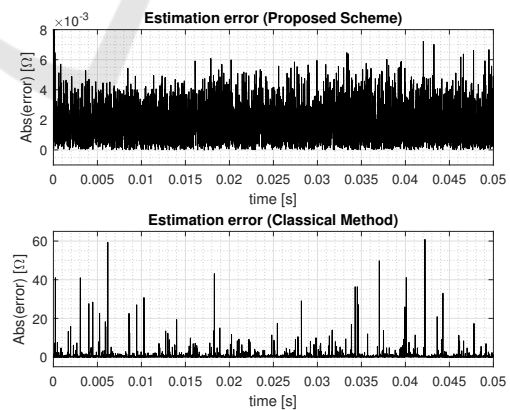


Figure 14: Estimation errors.

has a much bigger estimation error than the proposed scheme. The sliding mode-based scheme (SMS) outperforms the classical approach.

5 CONCLUSIONS

The sliding mode RLS based scheme for electrolytic capacitor condition monitoring proposed in this pa-

per is capable of estimating the equivalent series resistance (ESR) on-line despite noisy measurements. A constant forgetting factor has been used in the RLS algorithm since the ESR is a slowly time-varying parameter. Robust sliding mode differentiation has been satisfactorily applied for calculating signals required by the RLS algorithm.

The new condition monitoring approach outperforms an equivalent scheme based on linear approximation differentiators and the RLS with forgetting factor algorithm. The scheme is relatively simple in its form and design. A detailed design example has illustrated the simplicity of the method. Moreover, computer simulation results have demonstrated the effectiveness of the new capacitor condition monitoring scheme in which the degradation of an electrolytic capacitor on a DC-DC buck converter has been considered as proof of concept.

REFERENCES

- Abdennadher, K., Venet, P., Rojat, G., Retif, J. M., and Rosset, C. (2008). A real time predictive maintenance system of aluminium electrolytic capacitors used in uninterrupted power supplies. In *2008 IEEE Industry Applications Society Annual Meeting*, pages 1–6.
- Abdennadher, K., Venet, P., Rojat, G., Retif, J. M., and Rosset, C. (2009). Kalman filter used for on-line monitoring and predictive maintenance system of aluminium electrolytic capacitors in UPS. In *IEEE Energy Conversion Congress and Exposition*, pages 3188–3193.
- Alwitt, R. and Hills, R. (1965). The chemistry of failure of aluminum electrolytic capacitors. *IEEE Transactions on Parts, Materials and Packaging*, 1(2):28–34.
- Amaral, A. M. R., Buatti, G., Ribeiro, H., and Cardoso, A. (2007). Using DFT to obtain the equivalent circuit of aluminum electrolytic capacitors. In *7th Int. Conf. on Power Elect. and Drive Systems*, pages 434–438.
- Buiatti, G. M., Amaral, A. M. R., and Cardoso, A. J. C. (2007a). ESR estimation method for DC/DC converters through simplified regression models. In *IEEE Ind. Applications Annual Meeting*, pages 2289–2294.
- Buiatti, G. M., Amaral, A. M. R., and Cardoso, A. J. M. (2007b). Parameter estimation of a DC/DC buck converter using a continuous time model. In *European Conf. on Power Elect. and Applications*, pages 1–8.
- Celaya, J. R., Kulkarni, C., Biswas, G., Saha, S., and Goebel, K. (2011). A model-based prognostics methodology for electrolytic capacitors based on electrical overstress accelerated aging. In *Proc. of the Conf. of the Prognostics and Health Management Soc.*
- Filippov, A. F. (1988). *Differential Equations with Discontinuous Righthand Sides*. Kluwer Acad. Publishers.
- Hewitt, D. A., Green, J. E., Davidson, J. N., Foster, M. P., and Stone, D. A. (2016). Observation of electrolytic capacitor ageing behaviour for the purpose of prognostics. In *Proc. of the 42nd Conf. of the IEEE Ind. Elect. Society (IECON 2016)*.
- Imam, A. M., Habetler, T. G., Harley, R. G., and Divan, D. (2005). Failure prediction of electrolytic capacitor using DSP methods. In *20th IEEE Applied Power Elect. Conf. and Exp.*, volume 2, pages 965–970.
- Isermann, R. and Münchhof, M. (2011). *Identification of Dynamic Systems: An Introduction with Applications*. Springer-Verlag.
- Kalman, R. E. (1960). A new approach to linear filtering and prediction problems. *Transactions on the ASME-Journal of Basic Engineering*, 82:35–45.
- Kulkarni, C., Biswas, G., Koutsoukos, X., Celaya, J., and Goebel, K. (2010). Experimental studies of ageing in electrolytic capacitors. In *Proc. of the Conf. of the Prognostics and Health Management Soc.*, pages 1–7.
- Kulkarni, C. S., Celaya, J. R., Biswas, G., and Goebel, K. (2012). Accelerated aging experiments for capacitor health monitoring and prognostics. In *IEEE AUTO-TESTCON Proceedings*, pages 356–361.
- Levant, A. (1993). Sliding order and sliding accuracy in sliding mode control. *Int. J. of Control*, 58(6):1247–1263.
- Levant, A. (1998). Robust exact differentiation via sliding mode technique. *Automatica*, 34(3):379–384.
- Livne, M. and Levant, A. (2014). Proper discretization of homogeneous differentiators. *Automatica*, 50(8):2007–2014.
- Ljung, L. (1999). *System Identification - Theory for the User*. Prentice-Hall, 2nd edition.
- Mendel, J. M. (2008). *Lessons in Estimation Theory for Signal Processing, Communications, and Control*. Pearson Technology Group, 2nd edition.
- Nichicon Corporation ((n.d.)). *Technical Notes on Aluminum Electrolytic Capacitors*. Tech. Note 8101E.
- Shtessel, Y., Edwards, C., Fridman, L., and A., L. (2014). *Sliding Mode Control and Observation*. Birkhäuser.
- Soliman, H., Wang, H., and Blaabjerg, F. (2016). A review of the condition monitoring of capacitors in power electronic converters. *IEEE Tran. on Ind. Applications*, 52(6):4976–4989.
- Wang, G., Guan, Y., Zhang, J., Wu, L., Zheng, X., and Pan, W. (2012). ESR estimation method for DC-DC converters based on improved EMD algorithm. In *Proc. of the IEEE Prognostics and System Health Management Conf.*, pages 1–6.
- Wang, H. and Blaabjerg, F. (2014). Reliability of capacitors for DC-link applications in power electronic converters: An overview. *IEEE Trans. on Ind. App.*, 50(5):3569–3578.
- Zhuang, W. (1998). RLS algorithm with variable forgetting factor for decision feedback equalizer over time-variant fading channels. *Wireless Personal Communications*, 8(1):15–29.